Performance of wire mesh mist eliminator

Hisham T. El-Dessouky [a,*], Imad M. Alatiqi [a], Hisham M. Ettouney [a], Noura S. Al-Deffeeri [b]

[a] *Chemical Engineering Department, Kuwait University, P.O. Box 5969, Safat, Kuwait*
[b] *Ministry of Electricity & Water, Kuwait, Kuwait*

Abstract

An experimental study was made to measure the performance of wire mesh mist eliminator as a function of broad ranges of operating and design conditions. The experiments were carried out in an industrial scale layered type demister pad made of 316 L stainless steel wires. The demister performance was evaluated by droplet separation efficiency, vapor pressure drop of wet demister, and flooding and loading velocities. These variables were measured as a function of vapor velocity (0.98–7.5 m/s), packing density (80.317–208.16 kg/m^3), pad thickness (100–200 cm), wire diameter (0.2–0.32 mm), and diameter of captured droplets (1–5 mm). All the measurement results lie in ranges where, in practice, the wire mesh mist eliminator predominates. The experimental results indicate that the separation efficiency increases with both the maximum diameter of capture water droplets and the vapor velocity and with the decrease of wire diameter. The pressure drop for the dry demister is relatively low and depends only on the vapor velocity. The pressure drop increases linearly up to the loading point, thereafter; the rate of increase is larger. Beyond the flooding point, the increase rate is significant even for the slightest rise in the vapor velocity. The flooding velocity diminishes with the beef-up of the packing density and with the decrease of the wire diameter. Three empirical correlations were developed as a function of the design and operating parameters for the separation efficiency, pressure drop for the wet demister in the loading range, and the flooding and loading velocities. These correlations are sufficiently accurate for practical calculations and demister design. The temperature depression corresponding to the pressure drop in a wire mesh mist eliminator systems installed in a typical multi stage flash desalination plant was estimated from the developed correlation. A good agreement was obtained between the design values and the correlation predictions. © 2000 Elsevier Science S.A. All rights reserved.

Keywords: Mist eliminator; Wire mesh; Droplet separation; Evaporation; Thermal desalination processes

1. Introduction

Wire mesh mist eliminator, in the most general sense, is a simple porous blanket of metal or plastic wire retains liquid droplets entrained by the gas phase. The separation process in the wire mesh mist eliminator includes three steps; the first, being 'inertia impaction' of the liquid droplets on the surface of wire. As the gas phase flows past the surface or around wires in the mesh pad the streamlines are deflected, but the kinetic energy of the liquid droplets associated with the gas stream may be too high to follow the streamline of the gas and they impinged on the wires. The second stage in the separation process, is the coalescence of the droplets impinging on the surface of the wires. In the third step, droplets detach from the pad. In the vertical-flow installations, the captured liquid drains back in the form of large droplets that drip from the upstream face of the wire mesh pad. In the horizontal flow systems, collected liquid droplets drain down through the vertical axis of the mesh pad in a cross flow fashion.

There are a number of industrial processes wherein the liquid and the gas phases come into intimate direct contact with each other as a part of the process. As a result of viscous and aerodynamic forces, liquid droplets of various sizes are entrained and carried along with the moving gas stream. In most instances, it is

* Corresponding author. Tel.: + 965-4811-1188 (ext. 5613); fax: + 965-483-9498.

E-mail address: eldessouky@kuc01.kuniv.edu.kw (H.T. El-Dessouky)

desirable or even mandatory that these droplets be removed from the gas stream for different reasons. Examples of such considerations are recovery of valuable products, improving emission control, protection of downstream equipment, and improving product purity. A typical use of mist eliminator takes place in such operations as distillation or fractionation, gas scrubbing, evaporative cooling, evaporation and boiling, trickle equipment for sewage and the like.

There are several devices which are offered to industry for separating the entrained liquid droplets and each of which are effective over their own particular range of mist size. Mist eliminators can be summarized into the following groups settling tanks, fiber filtering candles, electrostatic precipitators, cyclones, impingement van separators, and wire mesh.

In the early days of evaporators, especially in thermal desalination plants, the solid vane type separators were used. However, the system suffers from the following drawbacks: (1) high pressure drop (which could result in the total loss of temperature driving force between stages) and (2) excessive brine carry over. Today, the wire mesh mist eliminator is widely used in thermal desalination plants to remove the water droplets, which may be entrained with the boiled or/and flashed off vapor. This water droplet must be removed before the vapor condensation over the condenser tubes. If the mist eliminator does not separate efficiently the entrained water droplets, it will cause the reduction of distilled water quality and the formation of scale on the outer surface of the condenser tube. The last effect is very harmful because it reduces the heat transfer coefficient and enhances the corrosion of the tube material.

The main features of wire mesh mist eliminators are low pressure drop, high separation efficiency, reasonable capital cost, minimum tendency for flooding, high capacity, and small size. The performance of wire mesh eliminators depends on many design variable such as supporting grids, vapor velocity, wire diameter, packing density, pad thickness, and material of construction. Because the wire-mesh is not rigid, it must be supported on suitable grids. To obtain minimum pressure drop, maximum throughput, and maximum efficiency, the support grids must have a high percentage of free passage. To take full advantage of the 98% or so free volume in the wire-mesh, the free passage through the support grids should be greater than 90%. If the free passage through the support grids is much below 90%, the accumulated liquid is prevented from draining back through the support grids, causing premature flooding [1].

Typically, maximum allowable velocity for a mist eliminator is limited by the ability of the collected liquid to drain from the unit. In vertical up flow mesh demister, when the gas velocity increases past design levels, liquid begins to accumulate in the bottom of the unit. The liquid buildup results in re-entrain of the downstream. This is because the inertia of the incoming gas prevents the liquid from draining out of the unit. In horizontal units, the gas inertia pushes the captured liquid toward the downstream face [2]. As a rule, smaller diameter wire targets collect smaller liquid droplets more efficiently. For example, a 10 μm wire removes smaller droplets than a 200 μm wire. However, a bed of 10 μm wires normally has the tendency to flood and re-entrain at much lower gas velocities than a bed of 200 μm wire. This is because the thinner wires provide dense packing that can trap the liquid by capillary action between the wires [3]. Interweaving of small diameter wires with larger diameter wire has been used often to tackle some of the most difficult mist removal problems. This design uses the metallic or plastic wires as a support structure to hold the fine wires apart. Even with this approach, the throughput capacity of the unit is limited, compared to that possible with conventional mesh. Special internal mesh geometry modifications are now available that allow these bi-component (that is, small-fiber and large-diameter wire mesh) configurations to operate at velocities essentially the same as conventional mesh designs. These ultra-high-efficiency designs can be substituted for conventional mesh and used, for example, in the dehydration towers of natural gas production plants, where even small losses of absorption chemicals, such as ethylene glycol, can be a significant operating expense [4].

Construction materials for the wires include metal, fiberglass, plastics or polymers such as polypropylene or Teflon. Recently, three new alloys have been made available in wire form, which routinely provide three to five times the service lives of the traditional materials. These are Lewmet 66, SX and Saramet. They can offer improved service depending on the temperature and acid concentration of the gas stream [1].

The basic concept and main features of the wire mesh mist eliminator have been discussed in a limited number of publications. Examples can be found in the studies by Holmes and Chen [2], Feord et al. [5], Buerkholz [6], Belden [7], Bhatia [8] and Tennyson [9]. The main objective of primordial investigators of wire mesh mist eliminator system, is comparing the separation efficiency of the wire mesh with that of other mist eliminator units. A complete review of the origin and early history of technical papers dealing with different mist eliminator systems are surveyed by Buerkholz [6]. He reported that, in order to prevent any re-entrain of the water droplets captured in the wire mesh pad, the gas phase velocity should be limited to 4–5 m/s. Additionally, he presented experimental data for the flooding load, the corresponding increase in pressure drop, and the fractional separation efficiency. In a dimensionless form the fractional degree of precipitation depends on

the Stokes, the Reynolds, and Euler numbers. Experimental analysis show that for large Reynolds numbers and in a large range of the Euler number, the inertial precipitation depends on the dimensionless precipitation parameter. Therefore, a simple approximation formula is given for the fractional degree of precipitation and the limiting droplet size for all types of separators [10].

Bradie and Dickson [11] discussed the factors governing the wire mesh demister, and in particular with their application to entrainment removal in pool boiling systems. They derived the separation efficiency of the demister pad from the collection efficiency for a single wire. This efficiency is used to determine the minimum vapor velocity as a function of droplet size. Correlations are developed for the single and two phase (dry and wet) pressure drop through the demister together with empirical formula relating the flooding point to the vapor and liquid velocities. They measured the pressure drop and flooding conditions for a series of demisters installed in a small 140 mm diameter wind tunnel. The tested demisters included the layered and spiral-wound configurations. All the experimental results were taken for air–water at atmospheric pressure and ambient temperature. No attempt has been made to use fluids with different properties or to operate the system at other conditions.

Feord et al. [5] reported that the method used to design and predict the performance of the mist eliminator units are deficient in their inability to predict the concentration of dispersed liquid in the outlet gas stream. This requirement must be specified in many industrial applications, distinctively in gas treatment processes. Accordingly, they proposed a mathematical model to specify the outlet concentration and droplet size distribution for knitted mesh mist pad. The model predicts variations in performance and the decrease in the separation efficiency with decreasing both the droplet size in the feed mixture and the gas velocity. Quantitative predictions of the flooding velocity compared with the experimental results measured for air–water system. The model offers the prospect of optimizing the pad construction to maximize the separation efficiency at a target pressure drop or designing to a maximum pressure drop. The main drawback of the models developed by Feord et al. [5] and Bradie and Dickson [11] is the need for complete information on the entrainment level and the droplet size spectra. This type of data is not always available in practical units. Measuring droplet size distribution, especially in the small size range, is quite difficult, costly, and prone to inaccuracies. It is usually practical to develop such data only in the laboratory or pilot plant. Moreover, in many realistic cases the droplet spectrum is highly dynamic and undergoes rapid changes due to any disturbance in the evaporation process. Also, the models developed by Feord et al. [5] and Bradie and Dickson [11] are tested only for air–water system.

Robinson and Homblin [12] presented detailed experimental work undertaken to demonstrate the collection of liquid aerosols in a helical coil as a function of aerosol size, gas velocity, tube diameter and number of coils. They compared the performance of this helical coils with that of a knitted mesh, a cyclone and a packed bed. They found that the performance of the helical coil demister is superior to the other systems. Nevertheless, the pressure drop for the knitted mesh system was to some extent lower than that of any one of the considered systems. Simple knockout drums, mist-pad knockout drums, impingement separators, cyclones filter-bed mist collectors, wet scrubbers, and electrostatic precipitators mist eliminator systems have been discussed thoroughly by Capps [13]. The discussion was intended to serve as a guide to proper mist eliminator selection. Bayley and Davies [14] reviewed the applications of knitted mesh demisters and presented typical design layouts. They developed a nomogram, which allows the process design engineers to quickly and accurately assess size and capacity of the required demister.

To the best of our knowledge, the only paper available in the open literature that deals with the application of the wire mesh mist eliminator in multi stage flash (MSF) water desalination units is that of Lerner [4]. He stated that the width of the flashing chambers is usually dictated by mist eliminator area requirements. They introduced two new types of mist eliminators. The first one is the mist master while the second configuration is the V-2000. Their capacities respectively, are two and three times those of conventional mesh pads. The application of these types in MSF units would allow for greater reduction in chamber size. Also they reported that both of mist master and V-2000 have been used in many field applications. However, these mist eliminators have not been used in the desalination area where other complex design considerations come into play.

In view of the previous discussion the following conclusions can be drawn:

1. We believe that the research on performance evaluation of the wire mesh mist eliminators in operating conditions similar to that dominating in evaporators, specially in thermal desalination systems, is still in an immature state.
2. The application of wire mesh mist eliminator in thermal desalination units is based on either an experience-based performance specification or data supplied by the demister manufacturers.
3. The available theoretical models devoted to the performance of the wire mesh mist eliminators are not adequate for implementing to the industrial units. Therefore, in this work the emphasis is laid more on the experimental investigation.

In the current study, the performance of wire mesh mist eliminator was investigated experimentally. The demister used was layered type and made of 316 L stainless steel wire. The demister performance was evaluated by the droplet separation efficiency, the wet vapor pressure drop, and velocities for flooding and loading. These variables were measured as function of vapor velocity, wire diameter, packing density, pad thickness, and the considered droplet diameter. All the measured data lie in a range where, in practice, the wire mesh mist eliminator predominates. While experimental data provide clearer understanding of the phenomena occurring in mist eliminators, the developed correlations offer the most promise of improving design practice.

2. Experimental apparatus and procedure

The experimental apparatus is schematically sketched in Fig. 1. The system components include a Plexiglas column, a direct contact condenser, water circulating pump, the wire mesh mist eliminator, and a hot water tank. The required steam is supplied from an electrical boiler with a power capacity of 45 kW. The boiler generates saturated steam with a maximum pressure of 16 bars. In all experiments this pressure is set at 2 bars. A water chiller is used to provide the direct contact condenser with cooling water.

The Plexiglas column has a 75 mm inside diameter and 1500 mm height. It is fitted with several connections for sampling the up and downstream vapors, measuring the pressure drop across the wire mesh pad, and measuring the absolute pressure inside the column. Another line is used to connect the steam flowing from the mist eliminator to the direct contact condenser. The hot water tank has an inside diameter of 150 mm and a height of 300 mm. The tank walls are made of 3 mm

thick stainless steel. The Plexiglas column is sealed very well to the tank by a stocky layer of silicon rubber. The direct contact condenser is a glass container with 10 liters capacity. Thick rubber stoppers are used to plug the container thoroughly at the top and the bottom. The pipes for the steam and cooling water are sufficiently submerged by water inside the condenser. This is necessary to insure intimate contact between the two phases and to prevent the escape of steam before complete condensation. The water circulating pump is a centrifugal type with submerged inlet and a power of 0.375 kW.

The wire mesh mist eliminator, the heart of the experimental unit, was formed of wires used in constructing the wire mesh mist eliminator in typical multi stage flash (MSF) desalination units. The wire diameter ranges from 0.2 to 0.32 mm and is made from Stainless steel 316 L. The wire was combed and flattened to give a double layer. Several of the double layered wires are used to form the demister, where the appropriate number is chosen to give the desired pad thickness. The pad is placed on an annular ring and a central support beam inside the column. The system was held at the required height by fixing the bottom support grid to the ring and beam. The free passage through the support grid was 93.5%. This is necessary to obtain minimum pressure drop, maximum throughput and maximum efficiency. If the free passage through the support grids is much below 90%, the accumulated liquid is prevented from draining back through the support grids, causing premature flooding [2]. The mesh pad was sized to be 3 mm larger than the column inside diameter to provide a sung fit and to minimize bypassing of the steam.

Demisters are usually specified by means of their Specific area A_s, packing density, ρ_p, and void fraction ε. These parameters are defined as:

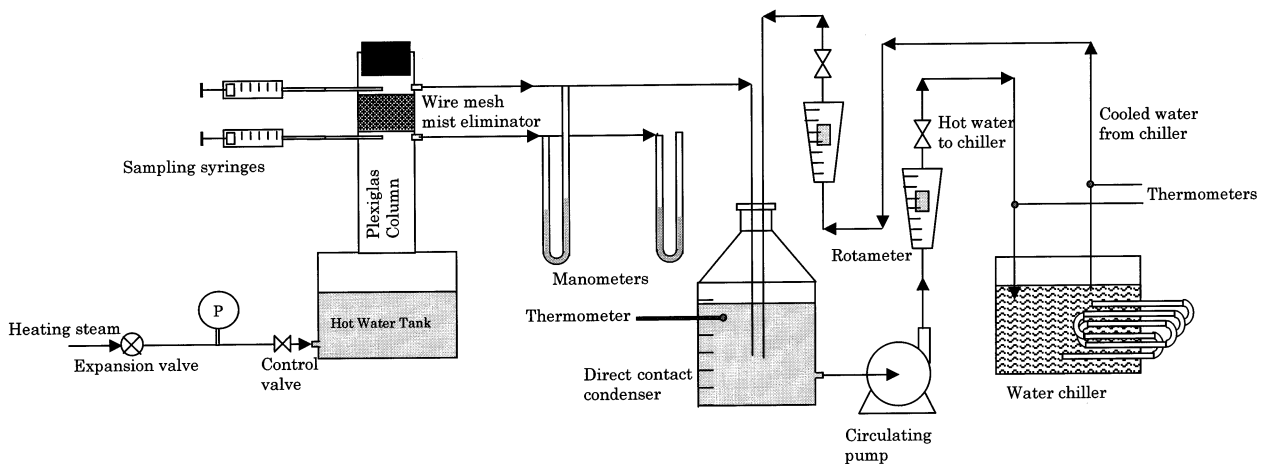$$A_s = \frac{\text{Surface area of wires}}{\text{Volume of demisters}} \quad (1)$$

Fig. 1. Schematic of experimental system.

$$\rho_{\mathrm{p}} = \frac{\text{Mass of wire}}{\text{Volume of demister}} \tag{2}$$

and

$$\varepsilon = 1 - \frac{\text{Volume occupied by wires}}{\text{Volume of demister}} \tag{3}$$

For industrial demisters A_{s} ranges from 140 to 300 m^2/m^3, ρ_{p} from 80 to 268 kg/m^3, and ε from 0.979 to 0.99 [15]. The characteristics of the demister pad used in the experiments are selected within the above ranges, where A_{s}, ρ_{p}, and ε were varied as follows: 150–294 m^2/m^3, 80–208 kg/m^3, and 0.974–0.990, respectively.

The measuring system consists of two water rotameters, three mercury glass thermometers, two vertical U-tube manometers, and a water level scale. Water flow rates to and from the direct contact condenser were measured by two calibrated water rotameters having an accuracy of approximately ±1%. Rotameters were calibrated by time–weight measurements. The three Mercury filled glass thermometers were used to measure the temperature of water flowing to and from the direct contact condenser and the temperature of condensed vapor inside the direct contact condenser. The resolution of these thermometers is ±0.1°C. The vertical U-tube manometer used to measure the pressure drop across the wire mesh was filled with water while the other manometer which is used to measure the absolute pressure inside the column was filled with Mercury. The accuracy of the manometers were 0.01 mmHg. The accuracy of the water level scale inside the direct contact condenser was ±1% of the full scale. Two identical syringes, with a 20 cm^3 capacity, were used for sampling the vapor flowing upstream and downstream the mist eliminator. The inside diameter of the syringe needle ranged from 1 to 5 mm. The size of the needle diameter gives a measure for the size of the largest collected droplet. The sampling processes by the two syringes were carried out simultaneously. Samples are withdrawn from the center of the Plexiglas column iso-kinetically, where the vapor velocity in the needle inlet is the same as that in the column. The weights of the two syringes were measured before and after sampling by sensitive balance with an accuracy of ± 0.0005% of the applied load. The increase in the mass of the syringes represents the mass of water droplets per 20 cm^3 of vapor. This sampling technique is simple to apply, gives a direct in situ measurements of the maximum diameter of the captured droplets, and gives the mass instead of the volume of collected droplets. Thus, there is no need to account for the droplets collected inside the needle or on the walls of the cylinders and the syringes. It should be stressed that there is no any relationship between the maximum droplet diameter determined by the needle inside diameter and the particle size distribution and the mean particle diameter.

All experimental measurements were taken at steady-state conditions. In a typical run, the manometer readings were adjusted to zero values. The steam valve was opened and the steam is admitted into the water accumulation tank. The mass flow rate of steam was controlled to achieve the steam velocity inside the column, which ranges from 1 to 7.5 m/s. The lower limit is determined by the minimum vapor velocity for water entrainment. On the other hand, the steam boiler capacity and the flooding of the demister pad determine the upper limit. The flow rate and the temperature of the cooling water to the direct contact condenser was adjusted in order to control the vapor condensation temperature, consequently setting the pressure inside the Plexiglas column. The liquid level of water inside the direct contact condenser was kept constant by regulating the water flow rate from the direct contact condenser.

Data were recorded for each run after steady state conditions had been maintained for at least 10 min. An overall heat balance for the experimental apparatus was calculated after each test run. Collected data was discarded and the experiment was repeated, if the heat balance was in error by more than 5%.

The vapor velocity inside the column, V, was calculated from the following relationship:

$$V = \frac{4M_{\mathrm{S}}}{\rho_{\mathrm{v}}\pi d_{\mathrm{i}}^2} \tag{4}$$

where ρ_{v}, d_{i}, and M_{s} are the steam density, column inside diameter, and the mass flow rate of condensing vapor, respectively. Two different methods are used to evaluate M_{s}. The first uses the readings of the two rotameters measuring the flow rate of water flowing from and to the direct contact condenser. In the second method, the mass of steam condensed, M_{s}, is calculated from the following energy balance relationship:

$$M_{\mathrm{s}} = \frac{M_{\mathrm{o}} C_{\mathrm{p}}(T_0 - T_i)}{C_{p_{\mathrm{v}}}(T_s - T_i) + \lambda_{\mathrm{s}}} \tag{5}$$

where C_{p} and $C_{p_{\mathrm{v}}}$ are the specific heat at constant pressure of water and steam respectively, λ_{s} is the latent heat of evaporation at steam temperature T_{s}, M_{o} is the mass flow rate of water flowing from the condenser, and T is the temperature. Subscripts o and i denotes the outlet and inlet conditions respectively. The above equation is developed from the total heat balance over the direct contact condenser.

Any experimental procedure contains uncertainties, and error analysis is essential to attach significance to results. To estimate the uncertainties in the results presented in this work, the approach described by Barford [16] was applied. The overall uncertainly assigned to a given measurement is defined as the root-sum-square combination of the fixed error due to the instrumentation and the random error observed during

measurements. Exercising this procedure, the calculations indicated errors of 2.4% for temperature, 3.15% for flow rate, 2.73% for pressure drop, 2.31% for absolute pressure and 1.19% for liquid level. On the basis of these errors, the pressure drop of the wet demister, separation efficiency, and velocities for loading and flooding may depart by 4.6, 3.2 and 4.1% from the true values.

3. Results and discussions

Data required to evaluate or size a wire mesh mist eliminator system include the droplet separation efficiency, capacity, and the vapor side pressure drop. These three parameters are interrelated and should be evaluated simultaneously. Efficiency of mist eliminator can be presented either as fractional removal or as fractional penetration. The summation of the removal and penetration efficiencies is equal to unity. Separation efficiency is a measure to the fraction of droplets in the vapor swept out by the wire mesh mist eliminator and is given by

$$\eta = \frac{M_{in} - M_{out}}{M_{in}} \times 100 \tag{6}$$

where M_{in} and M_{out} are the mass of entrained water droplet by the vapor up and down stream the mist eliminator, respectively.

The capacity of a wire mesh mist eliminator is determined by the conditions of loading and flooding. Beyond the loading point, the liquid holdup is high enough to improve the separation efficiency. The demister should operate at a velocity higher than the loading velocity. Flooding occurs when the vapor velocity exceeds a critical value. To prevent flooding, the mist eliminator must be designed and sized so that the design velocity is below the critical flooding velocity.

Fig. 2 shows the measured separation efficiency as a function of the maximum diameter of captured droplets. Three sets of data are presented that correspond to three different velocities of the vapor. As is shown, all curves have similar trend, where the removal efficiency increases with the increase of maximum diameter of collected droplets and the vapor velocity. There are three different mechanisms for capturing the entrained droplets by the wire mesh pad. These are diffusion, interception, and inertial impaction. The diffusion mechanism, sometimes called Brownian motions, is significant only for the capture of submicron droplets at a very low gas velocity. Interception occurs for droplets with dimensions similar to or higher than the wire diameter. Inertial impaction occurs when the vapor is forced to change its direction around an object. In all experimental measurements, the maximum droplet size was 5 mm and the wire diameter ranged
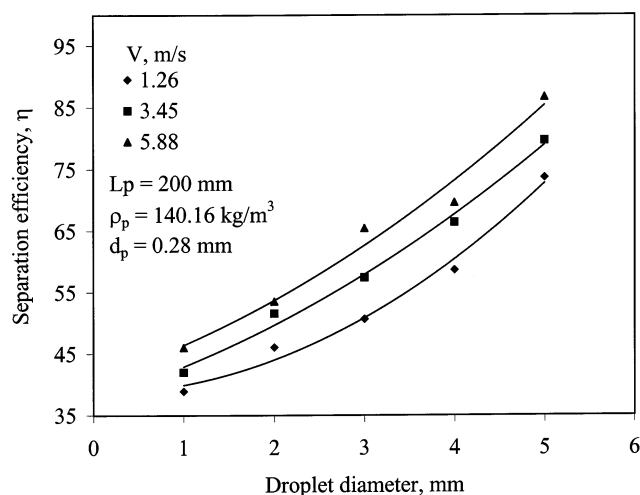

Fig. 2. Effect of droplet size on the separation efficiency at different values of vapor velocity.

from 0.2 to 0.32 mm. Thus, all these separation mechanisms are effective here; however, inertial impaction is clearly the predominant mechanism for droplet separation. As the vapor and entrained liquid droplets pass through the mist eliminator, the vapor phase moves freely, but, the liquid, due its greater inertia, is unable to make the required sharp turns. Therefore, the droplets are impacted and collected on the surface of the mesh wires. The droplet momentum or inertia is proportional to their velocity, mass, and diameter. Droplets with sufficient momentum can break through the vapor streamlines and continue to move in a straight line until they impinge on the target. The second stage in the separation process is the coalescence of the droplets, which impinge on the wire surface. Subsequently, the droplets compound and form streams or rivulets, which drain back against the vapor flow.
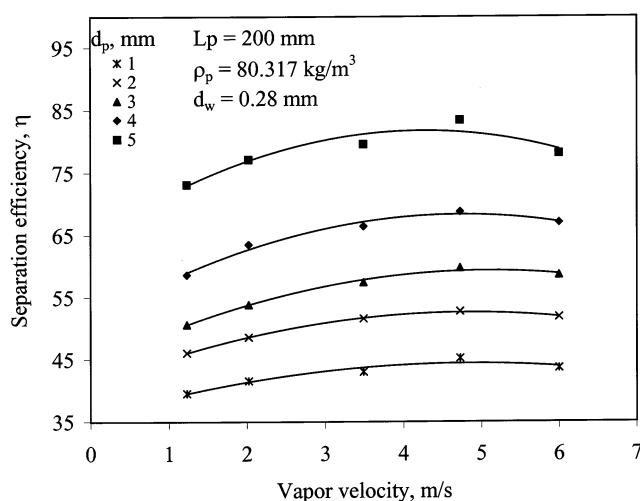

Fig. 3. Effect of vapor velocity on the separation efficiency at different values of droplet size.

Fig. 3 displays the variation of the separation efficiency with the vapor velocity at different values of maximum size of collected droplets. The separation efficiency increases steadily with the vapor velocity until it reaches a peak value and thereafter diminishes with further increase in vapor velocity. This observation can be attributed to re-entrainment of the water droplet with the vapor flowing inside the pad. There are three different forces controlling the movement of the water droplets accumulated within the demister pad. These are the drag, the gravity, and the surface tension forces. When the gravity force is dominant, the droplets are detached from the wire and drained by gravity. Re-entrainment of the collected water droplets with the vapor flowing in the demister occurs because the shearing energy per unit volume of liquid droplet is sufficient to create liquid droplets having a large ratio of surface to volume. This will increase the drag force exerted by the vapor on the droplets external surface. The drag force is proportional to the vapor interstitial velocity and droplets surface area and density. The vapor velocity in the pad increases at larger liquid hold up. This is because the liquid occupies part of the void fraction, thus, decreasing the available area for vapor flow. The liquid hold up in the pad is related to the rates of draining, re-entrainment, and collection. The increase in vapor velocity reduces the rate draining and increases the rates of collection and re-entrainment. Moreover, at high vapor velocities, the re-entrained liquid droplets can re-impact on the surfaces of subsequent wires. This may lead to the atomization of the water droplet by the force of the impact. Consequently, a very fine spray of droplets is generated, which is difficult to recapture by subsequent separators. This may explain the decrease in the separation efficiency at large vapor velocities.

The effect of the wire mesh diameter on the separation efficiency at different values of vapor velocity is displayed in Fig. 4. These results are obtained for a maximum droplet size of 5 mm, a pad thickness of 200 mm, and a packing density of 176.35 kg/m³. As displayed, the droplet separation efficiency improves with the decrease of the wire diameter. The influence of the wire diameter on the separation efficiency is more pronounced at lower vapor velocities. This is caused by the fact that the surface area of the wires at constant packing density and depth is directly related to the wire diameter. As a result, more droplets with smaller size can be trapped for mesh wires with smaller diameters, where number of liquid droplets touching the wire is primarily determined by the ratio between the wire diameter and the droplet size. Moreover, as the wire diameter is reduced, the surface area is increased. Therefore, a larger amount of entrained droplets are caught within the demister pad due to capillary action. At high vapor velocity, the shearing energy per unit
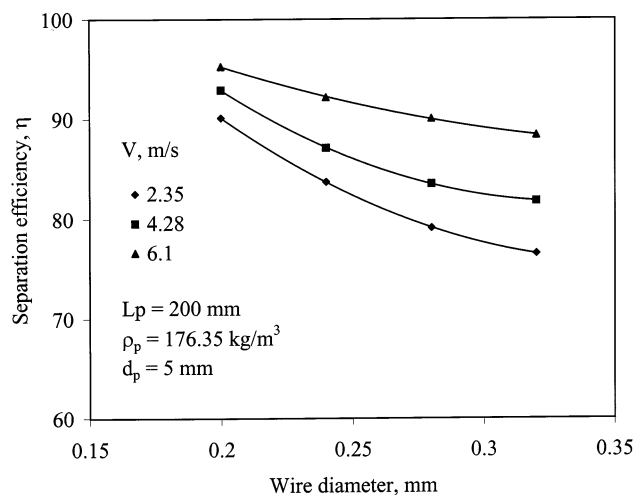

Fig. 4. Effect of wire diameter on the separation efficiency at different values of vapor velocity.

volume of the liquid droplets captured in the pad progressively increases as the wire diameter decreases. As a result, the liquid re-entrainment becomes excessive. Although, the results show the superior performance of demisters with smaller diameter wires; however, use of larger diameter wires is necessary to facilitate demister washing and cleaning. Also, use of larger diameter wires gives the demister adequate mechanical strength and operational stability.

The wire surface area for the wire mesh mist eliminator is directly related to the demister packing density. The increase of the pad packing density is associated with the reduction of the porosity of the pad. As a result, the number of entrained droplets which approaching the wires and the amount of captured droplets increases at larger surface area for the wires. This fact can be employed to explain the steady augmentation of the separation efficiency with the increase
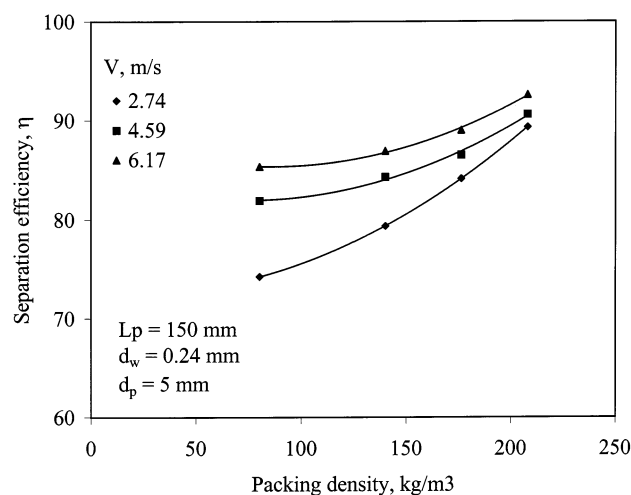

Fig. 5. Effect of packing density on the separation efficiency at different values of vapor velocity.

of the demister packing density as illustrated in Fig. 5. It is interesting to note that the effect of the pad density on the separation efficiency is more pronounced at low vapor velocities. This is mainly due to the increase in droplet re-entrainment and liquid hold up at higher vapor velocities.

Fig. 6 elucidates the effect of the pad thickness on the separation efficiency. As it can be seen, the separation efficiency is insensitive to the increase in the pad thickness. The pad thickness is a measure of how many times the vapor will consecutively impinge on a wire during its passage through the mesh pad. It was observed visually that a thin layer of water was accumulated on the bottom surface of the wires facing the vapor. This thin film acts as an extra droplet collection media. However, this layer does not penetrate through the wire mesh pad and is not affected by the pad thickness. This explains the insensitivity of the separation efficiency with the increase in the pad thickness.

The variation in the specific pressure drop for dry and wet demisters at different packing densities is shown in Fig. 7. The dry demister refers to the condition at which the pad is free of water droplets. On the other hand, the wet demister assigns the state at which the water droplets are retained inside the pad. As it can be seen, the pressure drop for the dry demister, in general, is relatively low and increases linearly with the vapor velocity. The pressure drop for the dry demister is a measure of the relative resistance of the fluid flow through the pad. This arises from the viscous drag between the vapor and the wires forming the demister pad and also because of kinetic energy loss due to the changes of the flow direction. The viscous drag force and the kinetic energy loss are directly related to the vapor velocity and the total surface area of the wires (wetted area). The flow resistance is comparatively low because of the high voidage of the demister. Measure-
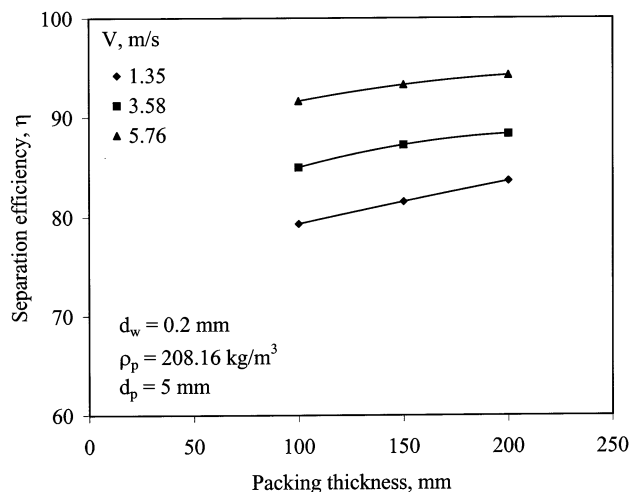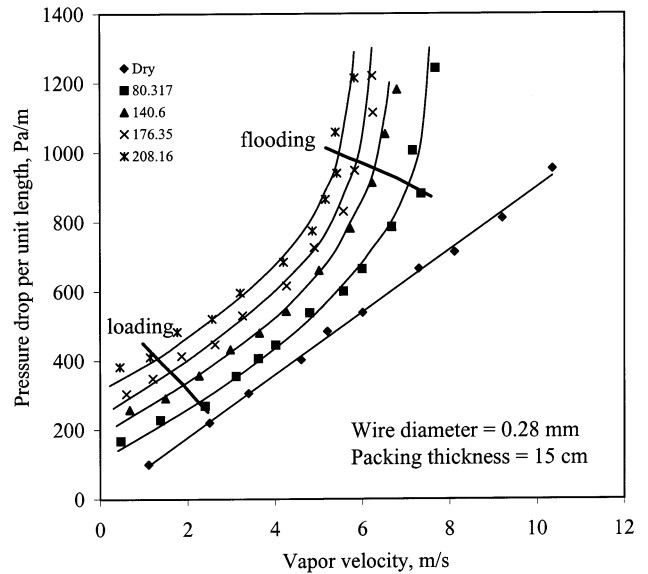

Fig. 7. Variation in pressure drop as a function of vapor velocity for different packing density.

ments show that the specific pressure drop for the dry demister is nearly independent of the demister thickness, density, and the wire diameter. The profiles for the specific pressure drop of the wet demister can be divided into three regions. The first occurs at low vapor velocities, where the specific pressure drop varies linearly with the vapor velocity and is parallel to the specific pressure drop of the dry demister. In the second region, the specific pressure drop increases more rapidly with the increase in the vapor velocity. In the third region, the pressure drop rises very steeply even with the slight increase of vapor velocity. The specific pressure drop in wet demisters is caused by the dry pad and due to the presence of water droplets. The pressure drop of the wet demister is complicated and there are three contributions to this pressure drop. The first term represents the frictional pressure drop because of the slip between the vapor phase and the demister pad. The second term represents the pressure drop due to the vapor phase acceleration. The last term accounts for the gravitational effects, which is smaller than the other two terms and can be safely neglected. The frictional and acceleration pressure drops are strongly dependent on the vapor velocity. The vapor velocity inside the demister is changed as a result of variations in the system operating parameters or due to the holdup of the liquid phase. As the liquid holdup progressively increases, the free space area available for the vapor flow decreases and results in rapid increase in the flow resistance. The liquid holdup may be either static or dynamic. Capillary action causes the static holdup and occurs at high retention of the liquid within the demister pad. The dynamic holdup takes place, as the settling velocity of the falling droplets becomes lower than the

Fig. 6. Effect of packing thickness on the separation efficiency at different values of vapor velocity.

upward vapor velocity. The static holdup increases with the increase of the wire surface area, which is directly related to the packing density.

Fig. 8 depicts variations of the specific pressure drop with the vapor velocity at different values of wire diameter. The figure illustrates that the pressure drop is inversely related to the wire size, which is caused by the increase of the wires surface area at smaller wire diameters. The static liquid holdup augments with the increase in the wires surface area. It is interesting to note that, the effect of wire diameter on the pressure drop is more pronounced at higher vapor velocities.

Variations in the specific pressure drop at loading and flooding conditions are shown in Figs. 7 and 8. Below the loading point the liquid holdup is relatively low and the vapor velocity does not significantly affect the pressure drop. Above the loading point, the liquid begins to accumulate or load the demister progressively causing the decrease of the free space for vapor flow. In this region, the pressure drop increases more rapidly with the increase in the vapor velocity. The flooding point represents the maximum loading the demister can accommodate. The flooding and loading points occur at lower vapor velocities upon the increase of the demister packing density and the decrease of the wire diameter. All these variables increase the surface area of wires forming the demister pad and consequently the extent of liquid holdup.

It is important to emphasize that the design capacity of most mist eliminators is determined by the phenomenon of re-entrainment. However, in thermal desalination processes, especially the multi stage flash (MSF) plants and the multiple effect evaporation (MEE) with large number of effects, the design capacity of the mist eliminator is obtained as a function of the

flooding points. The temperature difference available per stage in MSF plants is relatively small particularly when the number of stages is high. El-Dessouky and Bingulac [17] showed that the temperature depression corresponding to the pressure drop in the demister can considerably influence the plant thermal performance, specific heat transfer surface area and the specific cooling water flow rate. All these variables control the cost of desalinated water. It is worth mentioning that the flooding velocity is relatively lower than the re-entrainment velocity. Thus limiting the capacity of wire mesh mist eliminator by the flooding velocities will protect the heat transfer surface areas downstream the demister, prevent the diminishing of the product water quality, and minimize the thermodynamic losses. However, the vapor velocity must be higher than the loading point to ensure reasonable liquid holdup, which improves the separation efficiency.

3.1. Correlation of experimental results

In terms of the forgoing discussion, the separation efficiency of the wire mesh mist eliminator is affected by vapor velocity (V), wire diameter (d_w), droplet size (d_p), and packing density (ρ_p). On the other hand, the wet pressure drop is affected by the packing density (ρ_p), wire diameter (d_w), and vapor velocity (V). The flooding and loading velocities (V_f and V_l) are dependent on the packing density (ρ_p) and wire diameter (d_w).

The least square fitting of the experimental data gives the following empirical correlations:

$$\eta = 17.5047(d_w)^{-0.28264}(\rho_p)^{0.099625}(V)^{0.106878}(d_p)^{0.383197} \tag{7}$$

$$\Delta P = 3.88178(\rho_p)^{0.375798}(V)^{0.81317}(d_w)^{-1.56114147} \tag{8}$$

$$V_1 = 192.7189(\rho_p)^{-0.470865}(d_w)^{1.75578} \tag{9}$$

$$V_f = 128.358356(\rho_p)^{-0.287031}(d_w)^{1.220656} \tag{10}$$

The ranges of the experimental variables were V (0.98–7.5 m/s), ρ_p (80.317–208.16 kg/m³), L (100–200 mm), d_w (0.2–0.32 mm), and d_p (1–5 mm).

Figs. 9–12 show the comparison between the measured data and the calculated values from the developed correlations. The developed correlation predict the separation efficiency, η, the specific wet pressure drop, ΔP, and velocities of loading and flooding velocities, V_1 and V_f, with the following standard deviations 0.957, 0.9108, 0.9295 and 0.908, respectively.

3.2. Comparison with design data

The correlation for the specific wet pressure drop obtained in this study is used to predict the pressure drop and the associated temperature losses in the wire mesh demisters of the MSF plants in the Gulf states.
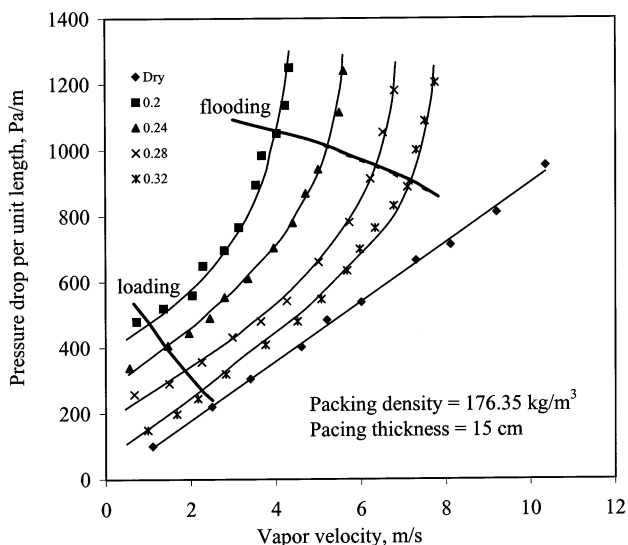

Fig. 8. Variation in pressure drop as a function of vapor velocity for different wire diameter.
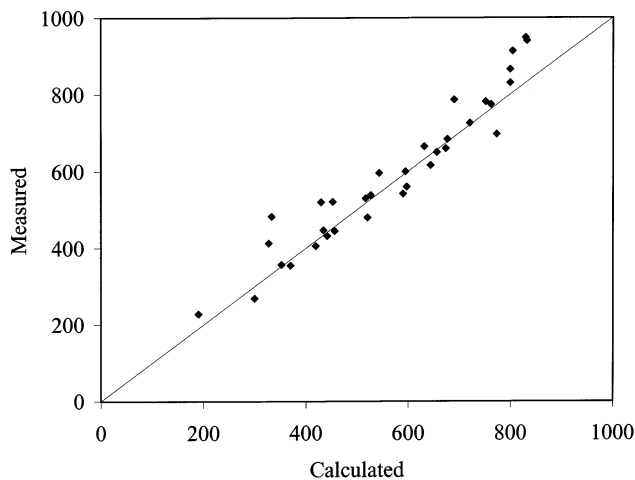
Fig. 9. Measured and calculated pressure drop per unit length.

The demister has a thickness of 150 mm, a packing density of 180.518 kg/m^3, and a wire diameter of 0.28 mm. Fig. 13 displays the comparison between the design temperature loss with the predicted values. As is shown, a good agreement is obtained between the design and model predictions. The temperature depression corresponding to the pressure drop in the demister is calculated from the relationship developed by El-Dessouky and Bingulac [17].

4. Conclusions

Research on evaluation of the performance of the wire mesh mist eliminator in operating conditions of MSF plants is still in an immature state. The available theoretical models devoted to simulation of the performance of the wire mesh pads are not adequate for implementation to the industrial units. This motivated execution of the present study, where experiments are
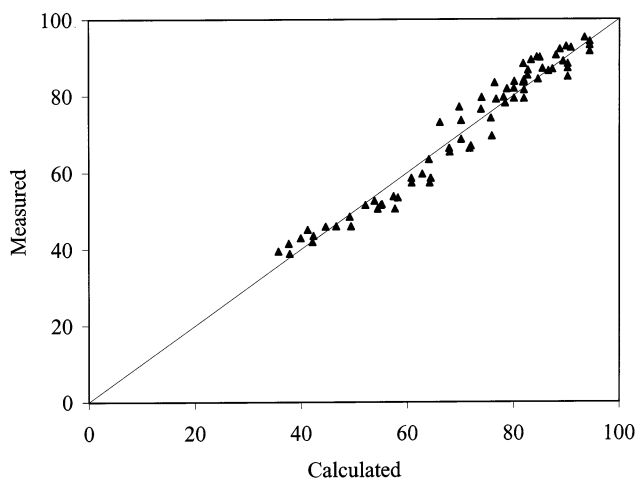

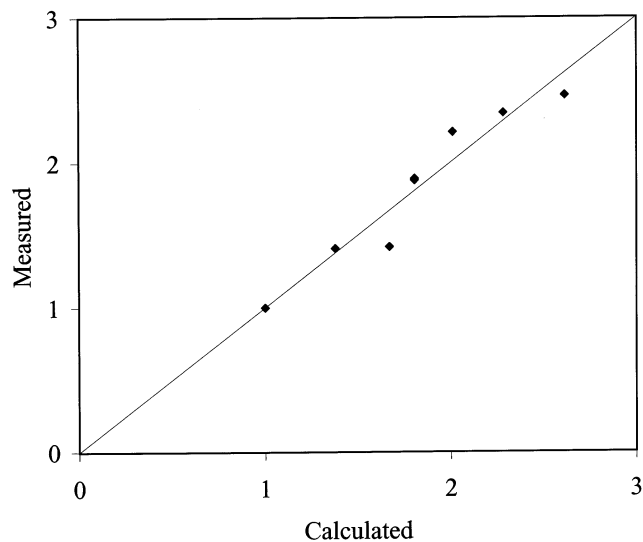Fig. 10. Measured and calculated separation efficiency.

Fig. 11. Measured and calculated loading velocity.

conducted to evaluate the performance of wire mesh demisters typical of MSF plants. The experimental measurements are made as a function of the vapor velocity, diameter of the wires, droplet diameter, packing density, and pad thickness. Collected data is used to analyze the system performance and to develop design correlations for the separation efficiency, the specific pressure drop for the wet demister, and the velocities for loading and flooding. Within the experimental range used, the following conclusions are made

1. The separation efficiency increases with the increase of the droplet size and the vapor velocity.
2. The specific pressure drop for the dry demister is low and varies linearly with the gas velocity.
3. The specific pressure drop for the wet demister increases linearly up to the loading point, thereafter,
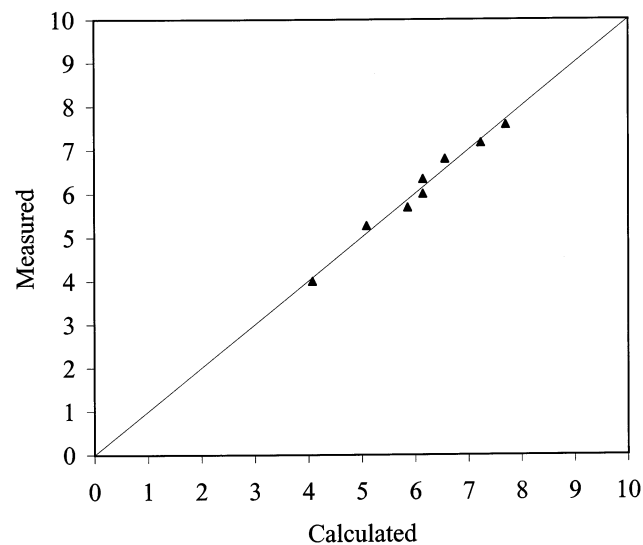

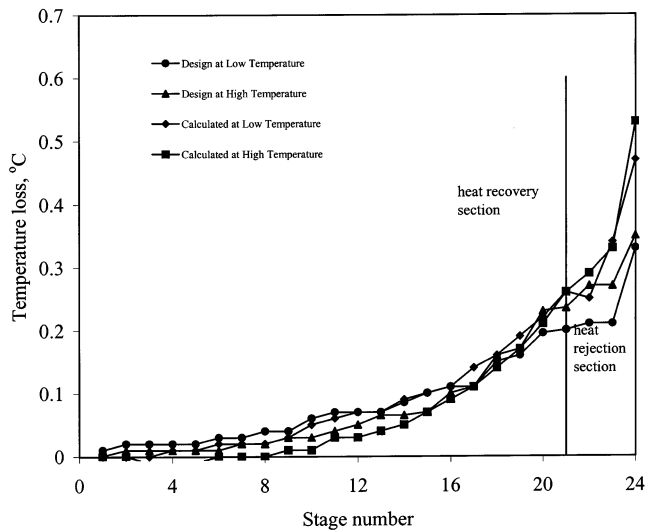Fig. 12. Measured and calculated flooding velocity.

Fig. 13. Comparison of design and calculated temperature losses in different flashing stages.

the rate of increase is higher. Beyond the flooding point, significant increase occurs in the specific pressure drop, even with the slightest increase in the vapor velocity.

4. The flooding and loading velocities increase at lower packing density and larger wire diameters.

Results and data analysis shows the new for further investigative research. Studies should consider performance evaluation of various demister designs, which may involve use of wires of different diameter within the same demister. Attention should be given to the effect of locating the demister pad with respect to the surface of the boiling or flashing liquid. Further studies concerning the static and dynamic hold up data will be helpful in better understanding of the demister performance.

Appendix A. Nomenclature

A_s	specific area, m^2/m^3
C_p	specific heat at constant pressure of water, $J/kg°C$
C_{p_v}	specific heat at constant pressure of steam, $J/kg°C$
d_p	maximum diameter of the captured droplets, mm
d_w	diameter of the wire, mm
d_i	column inside diameter, m
L	packing thickness, mm
M_0	mass flow rate of water flowing from the chiller, kg/s
M_{in}	mass of entrained water droplet by the upstream of the mist eliminator, kg/s
M_{out}	mass of entrained water droplet by the downstream of the mist eliminator, kg/s
M_s	mass of steam condensed, kg/s
t_i	Inlet temperature of water entering the chiller, °C
T_0	Outlet temperature of water leaving the chiller, °C
T_s	Steam temperature, °C
V	vapor velocity, m/s
ρ_v	vapor density, kg/m^3
ρ_p	packing density, kg/m^3
ε,	void fraction
λ_s	latent heat of evaporation at steam temperature, kJ/kg
η	droplet separation efficiency

References

[1] P. Fabian, R. Cusack, P. Hennessey, M. Neuman, Demystifying the selection of mist eliminators, Part I: The basics, Chem. Eng. 11 (1993) 148–156.

[2] T.L. Holmes, G.K. Chen, Design and selection of spray/mist elimination equipment, Chem. Eng. October (1984) 82–86.

[3] P. Fabian, P. Van Dessel, P. Hennessey, M. Neuman, Demystifying the selection of mist eliminators, Part II: The applications, Chem. Eng. December (1993) 106–111.

[4] B.J. Lenrner, High-tech mist elimination in multi-stage evaporators, Plant Operations Prog. 5 (1986) 52–56.

[5] D. Feord, E. Wilcock, G.A. Davies, A stochastic model to describe the operation of knitted mesh mist eliminators, computation of separation efficiency, Trans. IChemE. Res. Design 71 (1993) 282–295.

[6] A. Buerkholz, Droplet Separation, VCH, New York, 1989.

[7] R.D. Belden, Mist eliminators in evaporates and pans, Proceedings of SIA meeting, Savannah, GA USA, May, 1988, pp. 219–229.

[8] M.V. Bhatia, Entrainment separators, process equipment series, VCH, New York, 1989.

[9] R.P. Tennyson, Mist eliminator design and application, Proceedings of the 70th annual meeting of the air pollution control association, Toronto, Canada, June, 1977, pp. 20–24.

[10] A. Burkholz, Die Beschreibung der partikelabscheidung durch tragheitskrafte mit hilfe einer dimensionsanalytisch abgeleiteten kennzahl, Chem. Eng. Techol. 58 (1986) 548–556.

[11] I.K. Bradie, A.N. Dickson, Removal of entrainment liquid droplets by wire mesh demisters, Proc. Inc. Mech. Eng. 184 (1969) 195–203.

[12] K.S. Robinson, C. Homblin, Investigating droplet collection in helices and a comparison with conventional demisters, Filtration Separation May/June (1987) 166–171.

[13] W. Capps, Properly specify wire-mesh mist eliminators, Chem. Eng. Prog. (1994) 49–55.

[14] R.D. Bayley, G.A. Davies, Process applications of knitted mesh mist eliminators, Chem. Process. May (1973) 33–39.

[15] Anon, Selecting and sizing ACS mesh pad mist eliminators, Bulletin SA-12, ACS Industries, Inc., Houston, 1995.

[16] N.C. Barford, Experimental Measurements: Precision, Error and Truth, 2nd edition, Wiley, New York, 1990.

[17] H.T. El-Dessouky, S. Bingulac, Solving equations simulating the steady-state behavior of the multi-stage flash desalination process, Desalination 107 (1996) 171–193.